An SEIR epidemic model of fractional order to analyze the evolution of the COVID-19 epidemic in Argentina

Juan E. Santos, José M. Carcione, Gabriela B. Savioli, and Patricia M. Gauzellino

Abstract A pandemic caused by a new coronavirus (COVID-19) has spread worldwide, inducing an epidemic still active in Argentina. In this chapter, we present a case study using an SEIR (Susceptible-Exposed-Infected-Recovered) diffusion model of fractional order in time to analyze the evolution of the epidemic in Buenos Aires and neighboring areas (Región Metropolitana de Buenos Aires, (RMBA)) comprising about 15 million inhabitants. In the the SEIR model, individuals are divided into four classes, namely, susceptible (S), exposed (E), infected (I) and recovered (R). The SEIR model of fractional order allows for the incorporation of memory, with hereditary properties of the system, being a generalisation of the classic SEIR first-order system, where such effects are ignored. Furthermore, the fractional model provides one additional parameter to obtain a better fit of the data. The parameters of the model are calibrated by using as data the number of casualties officially reported. Since infinite solutions honour the data, we show a set of cases with different values of the lockdown parameters, fatality rate, and incubation and infectious periods. The different reproduction ratios R_0 and infection fatality rates (IFR) so obtained indicate the results may differ from recent reported values, constituting possible alternative

Juan E. Santos
School of Earth Sciences and Engineering, Hohai University, Nanjing 211100, China.
Universidad de Buenos Aires, Facultad de Ingeniería, Instituto del Gas y del Petróleo, Av. Las Heras 2214, Piso 3, Buenos Aires, Argentina.
Departmet of Mathematics, Purdue University. United States.
Tel.: +54-11-52850341. e-mail: santos@purdue.edu

José M. Carcione
National Institute of Oceanography and Applied Geophysics - OGS, Trieste, Italy.
School of Earth Sciences and Engineering, Hohai University, Nanjing 211100, China.

Gabriela B. Savioli
Universidad de Buenos Aires, Facultad de Ingeniería, Instituto del Gas y del Petróleo, Av. Las Heras 2214, Piso 3, Buenos Aires, Argentina

Patricia M. Gauzellino
Facultad de Ciencias Astronómicas y Geofísicas, Universidad Nacional de La Plata, Argentina

solutions. A comparison with results obtained with the classic SEIR model is also included. The analysis allows us to study how isolation and social distancing measures affect the time evolution of the epidemic.

1 Introduction

We present an SEIR subdiffusion model of fractional order ν, with $0 < \nu \leq 1$ to analyze the time evolution of the COVID-19 epidemic in Buenos Aires and neighboring areas (Region Metropolitana de Buenos Aires, (RMBA)) with a population of about 15 million inhabitants. The epidemic started officially on March 9th with the number of cases and deaths still increasing at July 15th. The classical SEIR model ($\nu = 1$) has been used by Carcione et al. [1] and Santos et al. [2] to model the COVID-19 epidemic in Italy and Argentina, respectively.

Fractional calculus has been used to define diffusion and wave propagation models in biological and viscoelastic materials [3, 4, 5, 6, 7, 8]. One important property of the fractional-order SEIR model is that incorporates memory and hereditary properties into the epidemic equations, a behavior exhibited by most biological systems. Among other authors that have applied fractional calculus to obtain solutions of the SEIR model, we mention Scherer et al. [9], that used a Grünwald-Letnikov time-discrete procedure, introduced by Ciesielski and Leszczynski [10] (CL method). Besides, Zeb et al. [11] presented an analysis of several numerical methods to solve the SEIR model of fractional order. For general works on fractional calculus including numerical methods, we refer to Podlubny [12] and Li and Zeng [13].

We first formulate an initial-value problem (IVP) for the SEIR subdiffusion equations of fractional order ν at the continuous level using the Caputo definition of the fractional derivative [5]. Existence and uniqueness of the solution of this IVP, with positive values, is demonstrated in [11]. The numerical solutions of the continuous IVP are computed by using the time-explicit algorithm of Gorenflo-Mainardi-Moretti-Paradisi (GMMP method) [14, 15]. The conditional stability of the time-explicit GMMP method (and also of the CL method) was demonstrated by Murillo et al. [17] [see their equation (19)]. The validation of the GMMP method is performed by comparison of its results against those of the classic SEIR model and those of the fractional Adams-Bashford-Moulton method (ABM method) as defined in [13].

The parameters of the SEIR model are the birth and death rates, infection and incubation periods, probability of disease transmission per contact, fatality rate and initial number of exposed individuals. These parameters, together with the order of the fractional derivative, are obtained by fitting the number of fatalities officially reported. This is an inverse problem with an infinite number of solutions (local minima) honouring the data, which is solved by using a quasi-Newton technique for nonlinear least squares problem with the formula of Broyden-Fletcher-Goldfarb-Shanno [18]. The numerical simulations give an effective procedure to study the spread of the evolution of virus, analyze the effects of the lockdown measures and predict the peak of infected and dead individuals.

2 The Caputo derivative and initial value problems

For $0 < \nu \leq 1$, the time fractional Caputo derivative $D_c^{\nu}(u(t))$ is defined as [14, 15, 5]

$$D_c^{\nu}(f(t) = \frac{1}{\Gamma(1-\nu)} \int_0^t \left[\frac{\partial}{\partial f(\tau)}\right] \frac{d\tau}{(t-\tau)^{\nu}}, \tag{1}$$

where $\Gamma(\cdot)$ denotes the Euler's Gamma function.

Note that the Caputo derivatives of constant functions $f(t) = 1$ vanish and those of powers of t, $f(t) = t^k$ are

$$\frac{\Gamma(k+1)}{\Gamma(k-\nu+1)} t^{k-\nu}.$$

The advantage of using the Caputo derivative in Caputo-type IVP's is that the initial conditions are the same as those of the classical ordinary differential equations. For details on the Caputo derivative and its relation with the Riemann-Liouville fractional derivative we refer to [5].

To approximate the time-fractional Caputo derivative, we use a backward Grünwald-Letnikov approximation at time $t_n = n\Delta t, n = 0, 1, , \cdots$, with $f_n = f(n\Delta t)$, Δt being the time step, as follows [14, 15]:

$$D_c^{\nu}(f(t))|_{t_{n+1}} \approx \frac{1}{(\Delta t)^{\nu}} \sum_{j=0}^{n+1} (-1)^j c_j^{\nu} \binom{\nu}{j} f_{n+1-j}. \tag{2}$$

The coefficients

$$c_j^{\nu} = (-1)^j \binom{\nu}{j}$$

can be obtained in terms of Euler's Gamma function using the recurrence relation

$$\binom{\nu}{j} = \frac{\Gamma(\nu+1)}{\Gamma(j+1)\Gamma(\nu-j+1)} = \frac{\nu-j+1}{j} \binom{\nu}{j-1}, \quad \binom{\nu}{0} = 1. \tag{3}$$

The work by Abdullah et al. [16] presents an analysis of the fractional-order SEIR model formulated in terms of the Caputo derivative and its GMMP time discretization.

3 The classical and fractional-order SEIR models

The IVP for the classic SEIR system of nonlinear ordinary differential equations is

$$\begin{aligned}
\dot{S} &= f_1(S,E,I,R)(t) = \Lambda - \mu S(t) - \beta S(t)\frac{I(t)}{N(t)}, \\
\dot{E} &= f_2(S,E,I,R)(t) = \beta S(t)\frac{I(t)}{N(t)} - (\mu+\epsilon)E(t), \\
\dot{I} &= f_3(S,E,I,R)(t) = \epsilon E(t) - (\gamma+\mu+\alpha)I(t), \\
\dot{R} &= f_4(S,E,I,R)(t) = \gamma I(t) - \mu R(t),
\end{aligned} \tag{4}$$

with initial conditions $S(0), E(0), I(0)$ and $R(0)$. A dot above a variable indicates the time derivative, while $N(t)$ is the number of live individuals at time t, i.e., $N = S + E + I + R \leq N_0$. In (4), S is the number of individuals susceptible to be exposed while E is the number of exposed individuals, in which the disease is latent; they are infected but not infectious. Individuals in the E-class become infected (I) with a rate ϵ and infected become recovered (R) with a rate γ. People in the R class do not move back to the S class since lifelong immunity is assumed. Furthermore, $1/\gamma$ and $1/\epsilon$ are the infection and incubation periods, respectively, Λ is the birth rate, μ is the natural per capita death rate, α is the average fatality rate, and β is the probability of disease transmission per contact. All of these coefficients have units of 1/time. Because of the relatively short period of the epidemic, it is assumed that $\Lambda = \mu N$, so that the deaths balance the newborns.

Dead individuals $D(t)$ are computed as $D(t) = N_0 - N(t)$, so that the dead people per unit time $\dot{D}(t)$, can be obtained as [19]:

$$\dot{D}(t) = \alpha I(t). \tag{5}$$

Next, we reformulate the system (4) into a fractional-order system by using the Caputo derivative in (1):

$$\begin{aligned}
D_c^\nu S(t) &= f_1^\nu(S,E,I,R)(t) = \Lambda^\nu - \mu^\nu S(t) - \beta^\nu S(t)\frac{I(t)}{N(t)}, \\
D_c^\nu E(t) &= f_2^\nu(S,E,I,R)(t) = \beta^\nu S(t)\frac{I(t)}{N(t)} - (\mu^\nu+\epsilon^\nu)E(t) \\
D_c^\nu I(t) &= f_3^\nu(S,E,I,R)(t) = \epsilon^\nu E(t) - (\gamma^\nu+\mu^\nu+\alpha^\nu)I(t), \\
D_c^\nu R(t) &= f_4^\nu(S,E,I,R)(t) = \gamma^\nu I(t) - \mu^\nu R(t),
\end{aligned} \tag{6}$$

The reproduction ratio, R_0, indicates the number of cases induced by a single infectious individual. When $R_0 < 1$, the disease dies out; when $R_0 > 1$, an epidemic occurs. Al-Sheikh [20] analyzes the behavior of the SEIR models in terms of R_0. For the SEIR model, R_0 is given by [21]

$$R_0 = \frac{\beta^\nu \epsilon^\nu}{(\epsilon^\nu+\mu^\nu)(\gamma^\nu+\alpha^\nu+\mu^\mu)}. \tag{7}$$

The infection fatality rate (IFR) is defined as

$$\text{IFR } (\%) = 100 \cdot \frac{\alpha^\nu}{\alpha^\nu + \gamma^\nu} \approx 100 \cdot \frac{\alpha^\nu}{\gamma^\nu}, \tag{8}$$

where this relation holds at all times, not only at the end of the epidemic.

3.1 Time discretization

An explicit conditionally stable GMMP algorithm for the fractional order system (6) is formulated as follows [14, 15]:

$$S_{n+1} = -\sum_{j=1}^{m+1} c_j^\nu S(m+1-j) + S_0 \sum_{j=0}^{m+1} c_j^\nu + (\Delta t)^\nu f_1(S_n, E_n, I_n, R_n) \tag{9}$$

$$E_{n+1} = -\sum_{j=1}^{m+1} c_j^\nu E(m+1-j) + E_0 \sum_{j=0}^{m+1} c_j^\nu + (\Delta t)^\nu f_2(S_n, E_n, I_n, R_n) \tag{10}$$

$$I_{n+1} = -\sum_{j=1}^{m+1} c_j^\nu I(m+1-j) + I_0 \sum_{j=0}^{m+1} c_j^\nu + (\Delta t)^\nu f_3(S_n, E_n, I_n, R_n) \tag{11}$$

$$R_{n+1} = -\sum_{j=1}^{m+1} c_j^\nu R(m+1-j) + R_0 \sum_{j=0}^{m+1} c_j^\nu + (\Delta t)^\nu f_4(S_n, E_n, I_n, R_n) \tag{12}$$

The results of the GMMP method (9)-(12) will be validated against the solution of the classical SEIR model ($\nu = 1$) and the Adams-Bashford-Moulton (ABM) time-explicit scheme as defined in [13] and included in the Appendix.

4 Numerical results

4.1 Validation of the GMMP algorithm

The results of the GMMP algorithm are cross-checked with those of the ABM solver for the classical SEIR model ($\nu = 1$) and SEIR models of fractional orders $\nu = 1, 0.9$ and 0.8.

We use the following parameters, given in Chowel et al. [22] and used by Carcione et al. [1] to perform a parametric analysis of the model. Average disease incubation $1/\epsilon = 3$ days, infectious period $1/\gamma = 8$ days, induced fatality rate $\alpha = 0.006$/day, $\beta = 0.75$/day, and $\Lambda = \mu = 0$. The initial conditions are $E(0) = 1, S(0) = N(0) - E(0) - I(0), I(0) = 1$ and $R(0) = 0$. The time step is $dt = 0.01$ day and $\mathrm{N}_0 = 10$ million. This case corresponds to a high reproduction ratio $R_0 = 5.72$.

Figures 1–6 show the results of the four classes, S,E,I,R, and the dead and dead per day individuals computed by using the GMMP and ABM algorithms. First, an

excellent agreement between the results of the two algorithms is observed for all values of the fractional order derivative ν. In particular, the results for $\nu = 1$ agree with those of Figures 1 and 2 in [1]. Figure 1 shows that decreasing the order of the fractional derivative causes a delay and an increase in the number of susceptible individuals. While for the classical model the number of infectious individuals vanish at long times, this is not the case for the orders $\nu = 0.8$ and $\nu = 0.9$ (Figure 3). We run the simulator up to a very long time but the individuals do not vanish, so that the epidemic never ends (in theory). This happens because $R_0 \geq 1$. We run other examples with different parameters such that $R_0 < 1$ and as expected the number of infectious individuals vanish and the epidemic dies out. For brevity these plots are not shown.

Regarding the exposed infected classes (Figures 2-3), a decrease in ν causes delays and reduces the amplitude of the peaks of these classes. Furthermore, as ν decreases the number of casualties increase as seen in Figure 4 while Figure 6 shows a delay and increase of the peak in the number of dead individuals per day.

These simulations consider a single value of β, the lockdown parameter. In a realistic case, β is a function of time and the procedure is that every time β changes, the algorithm has to be fully initialized from the beginning. Changing β in the same time loop yields wrong results. This fact has been verified by cross-checking different algorithms and several fractional orders.

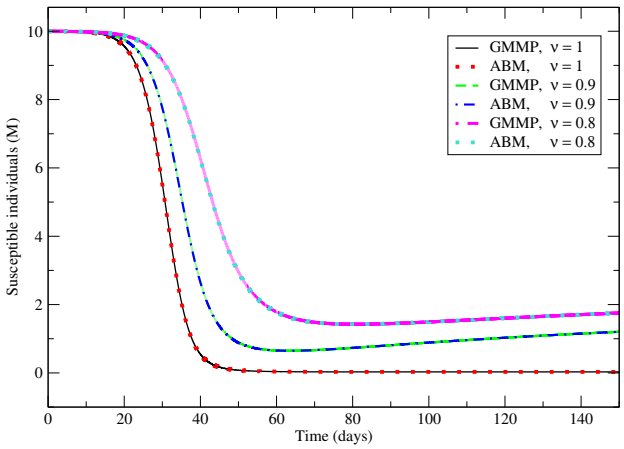

Fig. 1 Susceptible individuals for the classical SEIR model ($\nu = 1$) and fractional-order derivatives $\nu = 0.8$ and 0.9

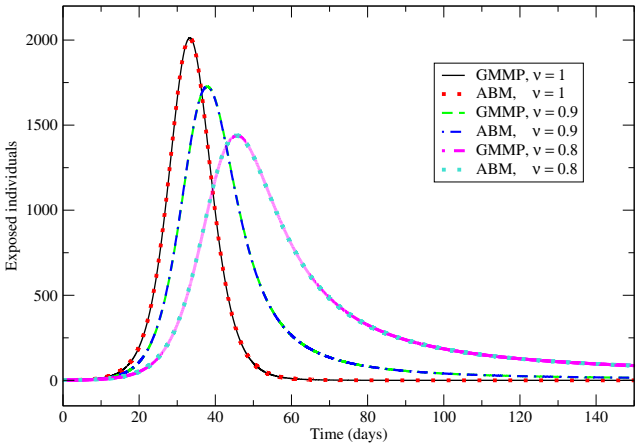

Fig. 2 Exposed individuals for the classical SEIR model ($\nu = 1$) and fractional-order derivatives $\nu = 0.8$ and 0.9

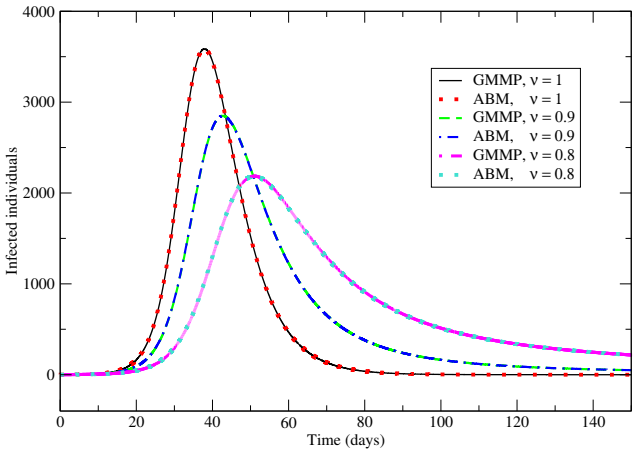

Fig. 3 Infected individuals for the classical SEIR model ($\nu = 1$) and fractional-order derivatives $\nu = 0.8$ and 0.9

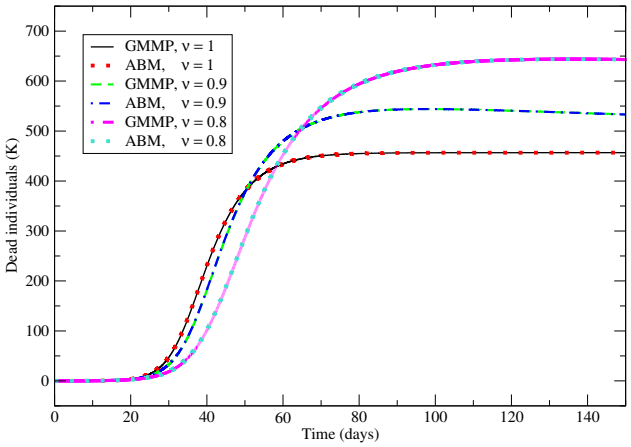

Fig. 4 Dead individuals for the classical SEIR model ($\nu = 1$) and fractional-order derivatives $\nu = 0.8$ and 0.9

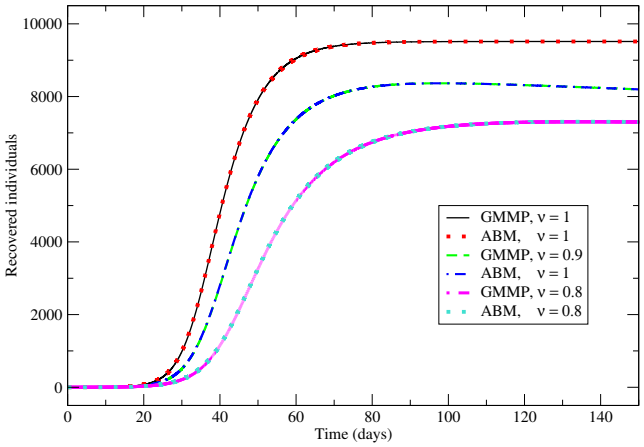

Fig. 5 Recovered individuals for the classical SEIR model ($\nu = 1$) and fractional-order derivatives $\nu = 0.8$ and 0.9

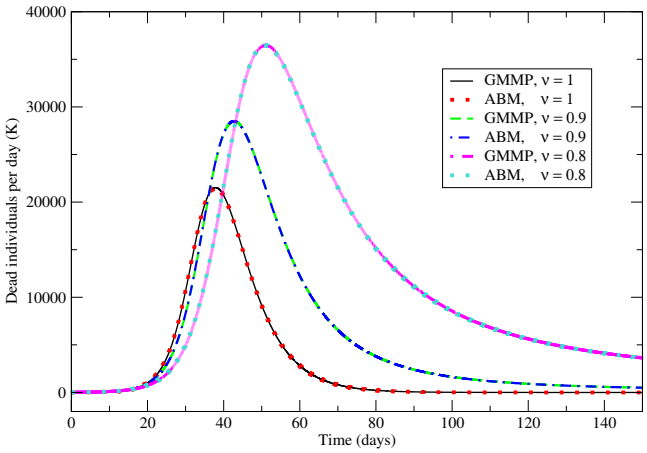

Fig. 6 Dead individuals per day for the classical SEIR model ($\nu = 1$) and fractional-order derivatives $\nu = 0.8$ and 0.9

5 Analysis of the COVID-19 epidemic in the RMBA

We model the COVID-19 epidemic in the RMBA, with a population $N_0 = 14839026$ individuals according to the 2010 Census (`https://www.indec.gob.ar/indec/web/Nivel4-Tema-2-41-135`). The prediction of the time evolution of the epidemic is very difficult due to the uncertainty of the parameters defining the SEIR model. Virus properties such as the infectious and incubation periods (γ^{-1} and ϵ^{-1}) and life expectancy of an infected individual (α^{-1}) lie in certain bounded intervals. Instead, the parameter β is time dependent, due to changes according to the lockdown and social-distance measures imposed by the government. Most authors use the infectious individuals to calibrate the model, e.g., González-Parra et al. [23], who model the AH1N1/09 influenza epidemic in Bogotá, Colombia and in the Nueva Esparta state in Venezuela.

Since the number of asymptomatic, undiagnosed infectious individuals in RMBA is unknown, we choose to calibrate the model with the number of officially reported casualties as the most reliable data, from day 1 (March 9, 2020) to day 120 (July 6th, 2020) (`https://www.argentina.gob.ar/coronavirus/informe-diario`). Concerning the parameters, fractional order and initial conditions of the model, we assume $\mu = 3.6 \times 10^{-5}$/ day, corresponding to a life expectancy of 76 years. Changes in the β parameter are associated with different measures of lockdown and social distance imposed by the goverment. Thus, we assume that β is a piecewise constant function, where its variations are related to the inflection points observed in the curve of casualties. After the initial time $t_0 = 1$

day, this curve shows two inflection points at times $t_1 = 31$ day and $t_3 = 50$ day. The fractional-order derivative ν, the values of α, β, ϵ, γ and the initial exposed individuals $E(0)$ are estimated by minimizing the L^2-norm between the simulated and actual casualties, which is an inverse problem with an infinite number of solutions due to the existence of local minima. The estimation is also performed for the classical case $\nu = 1$. This inverse problem is solved by using a quasi Newton approximation technique for nonlinear least-squares problems, based on the formula of Broyden-Fletcher-Goldfarb-Shanno [18]. Application of this technique to solve inverse problems in reservoir engineering can be found in [24]. Table 1 shows ranges of the fractional derivative ν, of the parameters α, β, ϵ, γ and the initial exposed individuals $E(0)$ used in the inversion procedure. Table 2 displays the initial values and results of three outputs (Cases) of the fitting procedure.

Table 1 Constraints and ranges of the estimation procedure

Variable →	ν	α^ν $(\text{day})^{-\nu}$	β^ν $(\text{day})^{-\nu}$	$(\epsilon^{-1})^\nu$ $(\text{day})^\nu$	$(\gamma^{-1})^\nu$ $(\text{day})^\nu$	$E(0)$
Lower bound	0.8	10^{-5}	0.1	3	3	10^2
Upper bound	1.0	10^{-1}	0.9	9	9	10^4

Let us analyze three cases, resulting from the minimization algorithm. We obtained the SEIR parameters, the fractional order and the initial exposed humans values fitting the data. In all the cases, the initial number of infected individuals is assumed to be $I(0) = 100$.

Figures 7 and 8 show the dead individuals and dead individuals per day for Case 1. The inflection point at $t_1 = 30$ day related to a change of R_0 from 2.37 to 0.986 shows a decay of the in the simulated curves, because of the effect of the lockdown. After $t_1 = 50$ day, the curves exhibits a continuous increase in casualties due to the relaxation of the lockdown measures with $R_0 = 1.441$. Figure 9 shows the behavior of all classes, with a a peak of 412 thousand infected individuals at day 210 (October 4th, 2020) while Figure 10 exhibit a death toll of 23000 after 800 days (May 17th, 2022) and at day 210 a peak of 230 casualties.

The parameters of Cases 2 and 3 in Table 2 also fit the data, with graphs similar to those in Figures 7 and 8. Case 2 predicts peaks of 1270 deaths and 619 thousand infected individuals at day 270 (December 3th, 2020). At day 800 (May 17, 2022), we have 109 thousand deaths and 7735 thousand recovered humans. This increase in numbers of infected individuals and casualties is due to the higher infection fatality rate IFR and higher reproduction ratios R_0 as compared with those of Case 1 (see Table 2).

Case 3, which corresponds to the classical SEIR model ($\nu = 1$), exhibits a peak of 140 casualties at day 207 and 397 thousand people infected. The end of the epidemic is consider the day at which the number of infected individuals is smaller than 1,

Table 2 Initial values and results of the estimation procedure.

Variable →	ν	α^ν (day)$^{-\nu}$	β_1^ν (day)$^{-\nu}$	β_2^ν (day)$^{-\nu}$	β_3^ν (day)$^{-\nu}$	$(\epsilon^{-1})^\nu$ (day)$^\nu$	$(\gamma^{-1})^\nu$ (day)$^\nu$	$E(0)$
Case 1								
Initial	0.92	6.00×10^{-4}	0.75	0.3	0.2	4.396	4.396	500
Optimum	0.932	5.589590×10^{-4}	0.427364	0.177402	0.259168	4.462195	5.579419	1258
R_0			2.377	0.986	1.441			
IFR =0.311								
Case 2								
Initial	0.85	6.00×10^{-4}	0.75	0.3	0.2	4.05	4.05	500
Optimum	0.869	2.039566×10^{-3}	0.501312	0.142112	0.242706	4.421400	6.589400	101
R_0			3.259	0.924	1.57			
IFR = 1.344								
Case 3								
Initial	1	6.00×10^{-4}	0.75	0.3	0.2	5.0	5.0	200
Optimum	1	3.573498×10^{-4}	0.633970	0.149269	0.213239	6.701927	6.780829	106
R_0			4.28	1.00	1.44			
IFR = 0.24								

which is day 724 (March 2nd, 2022) for this case. At this day, the total number of recovered and dead individuals are 7849 thousand and 19 thousand, respectively so that the total number of infected people at the end of the epidemic is 7868 thousand individuals. This is the case predicting the smallest number of casualties.

In the following, we compare the behavior of all classes for the different orders of the fractional derivative used in this analysis, i.e. $\nu = 1, 0.932$ and 0.869. Figure 11 displays the number of infected individuals, where there is a delay and increase of the peak values as the order of the fractional derivative decreases. This delay is consistent with that observed in Figure 3. Figure 12 shows an increase in the number of casualties by decreasing the order of the fractional derivative, with a 500 % increase between $\nu = 1$ and $\nu = 0.869$. Moreover, it can be seen that the curves stabilize at later times as the fractional order decreases. A similar effect is observed in Figure 13 for the recovered individuals. The curves exhibit asymptotic values at later times as ν decreases, and the lower the value of ν the later individuals recover

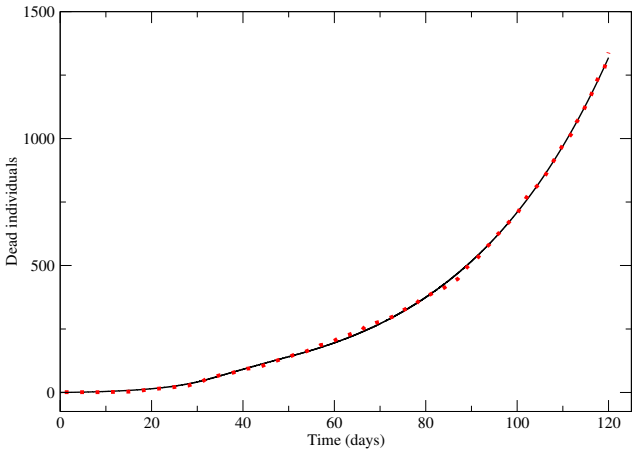

Fig. 7 Dead individuals. The red dots represent the data and the solid line the fit using the SEIR model of fractional order with $\nu = 0.932$

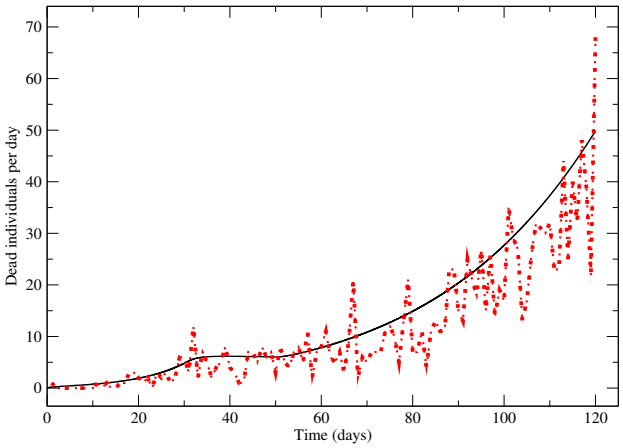

Fig. 8 Dead individuals per day. The red dots represent the data and the solid line the fit using the SEIR model of fractional order with $\nu = 0.932$

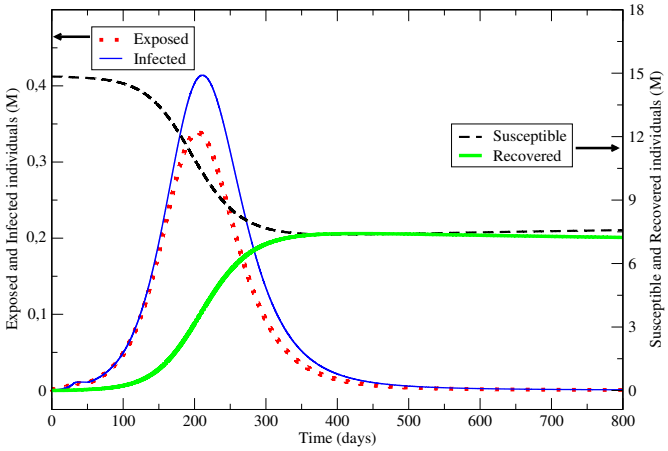

Fig. 9 Number of individuals in all classes (millions) for the SEIR model of fractional order with $\nu = 0.932$

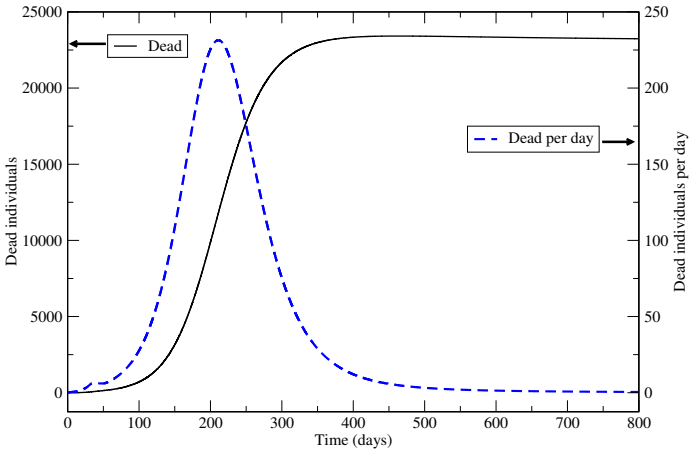

Fig. 10 Total number of deaths and deaths per day for the SEIR model of fractional order with $\nu = 0.932$

from the virus infection. Finally, Figure 14 shows that the decay of the number of susceptible humans is delayed as the value of ν decreases, indicating longer periods of the epidemic. Note that the general trends of Figures 11–14 are similar to those of Figures in Subsection 4.1, in spite of the fact that parameters obtained from the adjustment are different for the three cases.

As a general remark, we may state that when the order of the fractional derivative decreases, i.e., higher subdiffusion of the virus, the duration of the epidemic is extended, and the peak infected individuals and number of casualties increase.

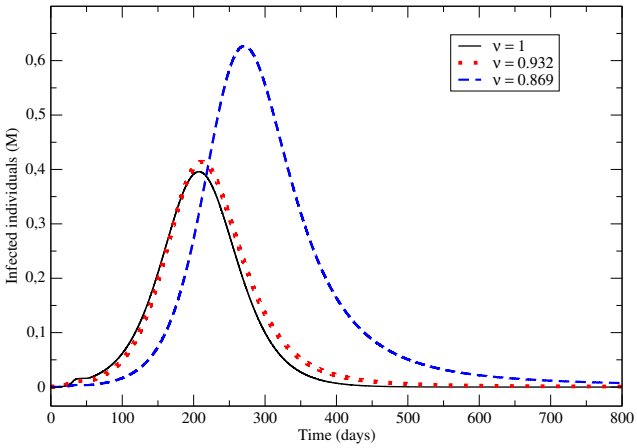

Fig. 11 Infected individuals for the SEIR model of fractional orders $\nu = 1, 0.932$ and 0.869

6 Appendix

The Adams-Bashford-Moulton explicit scheme for the fractional order SEIR equations is formulated as follows [13]

Predictor

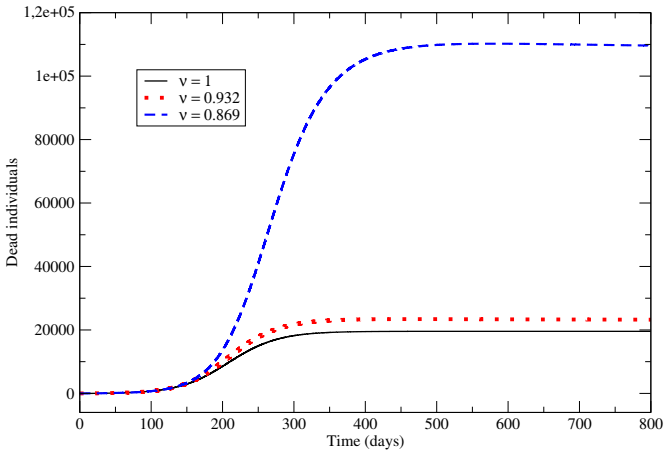

Fig. 12 Dead individuals for the SEIR model of fractional orders $\nu = 1, 0.932$ and 0.869

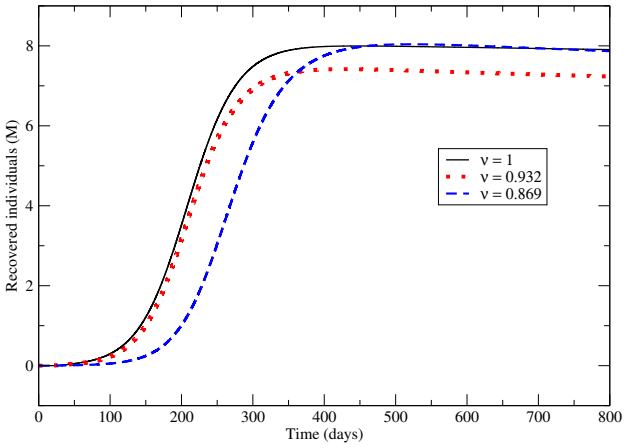

Fig. 13 Recovered individuals for the SEIR model of fractional orders $\nu = 1, 0.932$ and 0.869

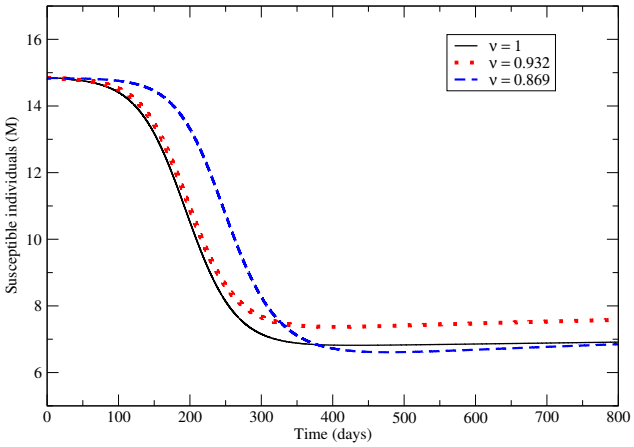

Fig. 14 Susceptible individuals for the SEIR model of fractional orders $\nu = 1, 0.932$ and 0.869

$$
\begin{aligned}
S^p_{n+1} &= ((n+1)\Delta t)S_0 + \sum_{j=0}^{n} b_{j,n+1)} f_1^{\nu}(S_j, E_j, I_j, R_j) \qquad (13)\\
E^p_{n+1} &= ((n+1)\Delta t)E_0 + \sum_{j=0}^{n} b_{j,n+1)} f_2^{\nu}(S_j, E_j, I_j, R_j)\\
I^p_{n+1} &= ((n+1)\Delta t)I_0 + \sum_{j=0}^{n} b_{j,n+1)} f_3^{\nu}(S_j, E_j, I_j, R_j)\\
E^p_{n+1} &= ((n+1)\Delta t)R_0 + \sum_{j=0}^{n} b_{j,n+1)} f_4^{\nu}(S_j, E_j, I_j, R_j)\\
N^p_{n+1} &= S^p_{n+1} + E^p_{n+1} + R^p_{n+1} + I^p_{n+1}.
\end{aligned}
$$

Corrector

$$S_{n+1} = ((n+1)\Delta t)S_0 + \sum_{j=0}^{n} a_{j,n+1} f_1^{\nu}(S_{n+1}^p, E_{n+1}^p, I_{n+1}^p, R_{n+1}^p)) \tag{14}$$

$$E_{n+1} = ((n+1)\Delta t)E_0 + \sum_{j=0}^{n} a_{j,n+1} f_2^{\nu}(S_{n+1}^p, E_{n+1}^p, I_{n+1}^p, R_{n+1}^p))$$

$$I_{n+1} = ((n+1)\Delta t)I_0 + \sum_{j=0}^{n} a_{j,n+1} f_3^{\nu}(S_{n+1}^p, E_{n+1}^p, I_{n+1}^p, R_{n+1}^p))$$

$$R_{n+1} = ((n+1)\Delta t)R_0 + \sum_{j=0}^{n} a_{j,n+1} f_4^{\nu}(S_{n+1}^p, E_{n+1}^p, I_{n+1}^p, R_{n+1}^p))$$

$$N_{n+1} = S_{n+1} + E_{n+1} + R_{n+1} + I_{n+1}.$$

In (13)-(14) the coefficients $b_{j,n+1)}, a_{j,n+1}$ are

$$b_{j,n+1} = \frac{1}{\Gamma(1+\nu)}\left[(n-j+1)^{\nu} - (n-j)^{\nu}\right]$$

$$a_{j,n+1} = \frac{1}{\Gamma(2+\nu)} = \begin{cases} (n)^{\nu+1} - (n-\nu)(n+1)^{\nu}, & j = 0, \\ (n-j+2)^{\nu+1} + (n-j)^{\nu+1} - 2(n-j+1)^{\nu+1}, & 1 \le j \le n-1 \\ 1, & j = n+1. \end{cases}$$

We refer to [16, 25, 13] for an error analysis and stability of the ABM method.

References

1. Carcione, J. M., Santos, J. E., Bagaini, C., and Ba, J., A simulation of a COVID-19 epidemic based on a deterministic SEIR model, Frontiers in Public Health, doi: 10.3389/fpibh.2020.00230, (2020) https://arxiv.org/abs/2004.035752004
2. Santos. J. E., Carcione, J M., Savioli, G. B., Gauzellino, P. M., Ravecca, A., and Moras, A., A numerical simulation of the COVID-19 epidemic in Argentina using the SEIR model, submitted to International Journal of Dynamics and Control (2020).
3. Mainardi, F., The fundamental solutions for the fractional diffusion-wave equation, Appl. Math. Lett., 9, 23-28 (1996).
4. Carcione J. M, Cavallini, F., Mainardi, F., and Hanyga, A., Time-domain seismic modeling of constant Q-wave propagation using fractional derivative, Pure Appl. Geophys.,159, 1719-1736 (2002).
5. Mainardi, F, Fractional calculus and waves in linear viscoelasticity, Imperial College Press, London (2010).
6. Caputo, M., Carcione, J. M. and Cavallini, F., Wave simulation in biological media based on the Kelvin-Voigt fractional-derivative stress-strain relation, Ultrasound in Med. Biol.,37 (6), 996-1004 (2011).
7. Caputo, M., and Carcione, J. M., Hysteresis cycles and fatigue criteria using anelastic models based on fractional derivatives, Rheologica Acta, 50, 107-115 (2011).
8. Carcione, J. M. and Mainardi, F., On the relation between sources and initial conditions for the wave and diffusion equations, Computers and Mathematics with Applications, 73, 906-913 (2017).

9. Scherer, R., Kalla S. L., Tang, Y. c and Huang, J., The Grünwald-Letnikov method for fractional differential equations, Computers and Mathematics with Applications, 62 902-917 (2011)
10. Ciesielski M. and Leszczynski J., Proc. 15th Conf. on Computer Methods in Mechanics (Wisla, Polonia), (2003) (arXiv:math-ph/0309007v1)
11. Zeb, A., Khan, M., Zaman, G., Momani, S. and Ertürk, V. S., Comparison of Numerical Methods of the SEIR Epidemic Model of Fractional Order, Z. Naturforsch., 69a, 81-89 (2014), DOI: 10.5560/ZNA.2013-0073
12. Podlubny, I., Fractional differential equations, San Diego, Academic Press, San Diego (1999).
13. Li, C., and Zeng, F, Numerical methods for fractional calculus, CRC press, Taylo & Francis Group, Boca Raton, (2015).
14. Gorenflo, R., Mainardi, F., Moretti, D., and Paradisi, P., Time fractional diffusion: A discrete random walk approach, Nonlinear Dyn., 29, 129-143 (2002).
15. Gorenflo, R., and Abdel-Rehim, E. A., Convergence of the Grünwald-Letnikov scheme for time-fractional diffusion, J. Comput. Appl. Math, 205, 871-981 (2007).
16. Abdullah, F. A., Liu, F., Burrage, P., Burrage, K. and Li, T., Novel analytical and numerical techniques for fractional temporal SEIR measles model, Numer Algor 79, 19-40 (2018) https://doi.org/10.1007/s11075-017-0426-6
17. Murillo, J. Q. and and Bravo Yuste, S. On three explicit difference schemes for fractional diffusion and diffusion-wave equations, Physica Scripta, T136 014025 (6 pp) (2000).
18. Gill, P., Murray, W., and Wright, M., Practical optimization. Academic Press, London, (1981).
19. De la Sen, M., Ibeas, A., Alonso-Quesada, S., and Nistal, R., On a new epidemic model with asymptomatic and dead-infective subpopulations with feedback controls useful for Ebola disease. Discrete Dynamics in Nature and Society (2017) https://doi.org/10.1155/2017/4232971
20. Al-Sheikh, S., Modeling and analysis of an SEIR epidemic model with a limited resource for treatment, Global Journal of Science Frontier Research, Mathematics and Decision Sciences, 12 (14) (2012).
21. Zhang, L. J., Li, Y., Ren, Q. and Huo, Z., Global dynamics of an SEIRS epidemic model with constant immigration and immunity, WSEAS Transactions on Mathematics, 12, 630-640 (2013).
22. Chowell, G., Fenimore, P. W., Castillo-Garsow, M. A., and Castillo-Chavez, C., SARS outbreak in Ontario, Hong Kong and Singapore: the role of diagnosis and isolation as a control mechanism, J. Theor. Biol., 224, 1-8 (2003).
23. González-Parra, G., Arenas, A. J. and Chen-Charpentier, B. M., A fractional order epidemic model for the simulation of outbreaks of influenza A(H1N1), Math. Meth. Appl. Sci., 37 2218-2226 (2014).
24. Savioli, G. B., and Bidner, M. S., Comparison of optimization techniques for automatic history matching. Journal of Petroleum Science and Engineering, 12(1) 25-35 (1994).
25. Li, C.P., Zhao, Z. G. and Chen Y. Q., Numerical approximation of nonlinear fractional differential equations with subdiffusion and superdiffusion, Comput. Math. Appl., 62, 855-875 (2011).